Production of Ultra-fine Metal Powder with Gas Atomization Processes

M. R. Wang†

Key Words: Metal Powder, Gas Atomization, Internal-Mixing, Internal Impinging, Substrate

Abstract

Experimental results of the metal powder production with internal mixing, internal impinging and the atomizer coupled with substrate design are presented in this paper. In a test with internal mixing atomizer, mean powder size was decreased from 37 μm to 23 μm for Pb65Sn35 alloy as the gas-to-melt mass ratio was increased from 0.04 to 0.17. The particle size further reduces to 16.01 μm as the orifice area is increased to 24 mm^2. The micrograph of the metal powder indicates that very fine and spherical metal powder has been produced by this process. In a test program using the internal impinging atomizers, the mean particle size of the metal powder was decreased from 22 μm to 12 μm as the gas-to-melt-mass ratio increased from 0.05 to 0.22. The test results of an atomizer coupled with a substrate indicates that the deposition rate of the molten spray on the substrate is controlled by the diameter of the substrate, the height of the substrate ring and the distance of the substrate from the outlet of the atomizer. This in turn determines the powder production rate of the spraying processes. Experimental results indicate that the deposition rate of the spray forming material decreases as the distance between the substrate and the atomizer increases. For example, the deposition rate decreases from 48% to 19% as the substrate is placed at a distance from 20 cm to 40 cm. On the other hand, the metal powder production rate and its particle size increases as the substrate is placed far away from the atomizer. The production of metal powder with mean particle size as low as 3.13 μm has been achieved, a level which is not achievable by the conventional gas atomization processes.

1. Introduction

Metal powders may be produced in large quantities by a variety of atomization techniques as referred to Cubberly et al[1] and Lavernia et al[2]. Particular methods are considered to produce metal powder for different metals, such as vibratory ball milling for aluminum, plasma arc spraying for tin, gas and water atomization for stannic. Rotating disk atomization (centrifugal atomization), vacuum atomization, and rotating electrode atomization are all applied in practice. Generally, people used water- and gas- atomization to produce metal powder. Controlling the gas flow and the pattern of the medium generally reduces efficiency. However, most atomizers are designed to allow the molten metal to fall freely and be controlled by the atomizing medium. Bradbury[3] reported that most used metal powders involve particles of sizes in the range of 175 mm to 43 mm. For special cases, particles must be superfine (<10 mm). For example, metal powder injection molding described by German[4] requires particle sizes lower than 20 mm. Liang[5] found that superfine metal powder can facilitate sintering materials up to 95% of the true density of a material with 3~8 μm surface roughness.

Metal powder production using gas atomization techniques has become popular in recent years. In an effort to develop the linear atomizer for the spray forming application, Samuelsen et al[6] characterized the performance of a linear atomizer on the 3003 aluminum alloy. They found that Aluminum powder size, SMD, decreases from 125 mm to 103 mm as atomization pressure increases from 310 kpa to 379 kpa. Anderson[7] studied the atomization of Ni-base alloy and found that atomizing at the deep gas-aspiration

†National Cheng Kung University, Taiwan
E-mail : Wangmr@mail.ncku.edu.tw

pressures (at condition of wake-closure) in close coupled gas atomizers yields the finest powder. Ting[8] further studied the wake closure phenomenon of melt atomization. They found that the wake-closure phenomenon (WCP) is highly sensitive to atomizer and melt pour tube geometry and pulsating atomization occurs. Stable wake-closure cannot be sustained during melt atomization. The melt filming process at above WCP gives rise to finer particle size distribution, lower melt flow rate, and higher GMR. Operating below WCP, the melt breakup mechanism could be similar to that of the free-fall atomization process.

The most popular atomizers utilized for metal powder production in the literature were the external mixing type[6-9]. For example, Mates et al[9] investigated the performance of the external mixing atomizer for the production of tin powder. An annular HPGA (converging) atomizer and an annular UNAL (converging and diverging) atomizer were used to investigate the atomization pergormance. The pressure ratios up to 29~51 are required to achieve the desired atomization. However, atomization on melt, using internal mixing atomizers, was extensively investigated by Wang et al[10]. Results show that the performance of this atomizer is better than the conventional one with an external atomization. The ultra-fine powder (SMD<13 μm) has been obtained under low pressure conditions and low gas-to-melt ratio at GLR=0.17 in the production of solder powder[11]. Wang et al[12] further optimized the nozzle design and control parameters using Taguchi method. Results indicate that the accumulative volume of the solder powder within 0~15 μm is 56.9%. That is, more than half of the powder is within extra-fine range, indicating the better performance for the production of the metal powder.

As a comparison, Wolf and Wilhelm[13] investigated the performance of atomizer with external-mixing mechanism, i.e., HPGA atomizer. The mean size of Tin particles is 60 mm to 35 mm as the atomization pressure between 8 bar to 70 bar. The gas-to-melt mass ratio jumps to 0.61~0.93, which is the typical case of the high mass flow rate for the external-mixing atomizer.

Investigation on the impingement of the spray jet has been the interests of many researchers due to its potential applications in industrial thermal control and material conditioning and processing. Angioletti et al[14] attempted to improve the local heat transfer rates by impinging jets. They found that the vortex stretched and increased the diameter as it approached the impinging plate. It turns out that the velocity of normal component tends to zero and the velocity of the radial component increases, becoming a larger vortex as it reaches the plate. They also found that the impact region is slightly offset with respect to the vertical position, due to the action of the stagnation region.

Atomization of molten metals into the metal spray becomes popular in recent development of the spray forming technology. Singer and Osprey[15,16] suggested that spray deposition was a new manufacturing process for metallurgy. The method has received considerable attention as it produces near-net-shape materials with uniform, rapidly solidified microstructure. Furthermore, superplastic property may be achieved by reducing the grain size for thermal mechanical processes (TMP). The grain size in most materials is less than 10 mm, but sometimes reaches 20 mm. Hence the finer atomization of the molten metal and its impact upon the solidification processes and the grain size is highly concerned.

In an effort to understand the deposition mechanisms of the spray forming material, Newbery et al[17] investigated the impingement of the metal spray on the flat and angled substrates. Dynamic properties of gas and the metal spray of Fe-0.8 wt.% C droplets during electric arc spraying was characterized by using particle image velocimetry (PIV). They found that flow behavior was dominated by the upward and then lateral flow of the numerous smaller droplets caused by splashing of superheated droplets on the substrate. At spray angles of 45° and greater, splash droplets are entrained exclusively in the 'downhill' flow of gas. When a topographic feature such a simple vertical step was introduced at the substrate, splash droplet behavior became complicated, with some splash droplets having trajectories that caused deposition on the vertical step wall.

As had been reported in the literature, the atomizers used in spray forming are of the free fall type with the

external gas impinging process. These atomizers are normally less efficient than those that are of the forced control type with the internal gas mixing process. The design of the atomizer with internal mixing atomization is hence adopted in this paper to improve the atomization performance for metal powder production. Furthermore, the particle size of the metal powder is controlled by the impingement of the spray on the substrate in the spray chamber. The combination of the metal powder production as well as the deposition of the spray forming material is performed.

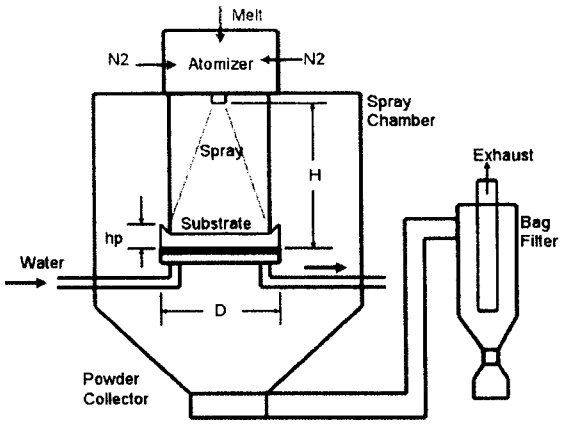

Fig. 1 Schematic of the experimental system

2. Experimental facility

Fig. 1 shows the schematic of the experimental system. The melt is first atomized by a twin-fluid atomizer. The metallic spray injected from the swirling chamber of the atomizer is then impinged upon the substrate to form the two phase impinging flow. Part of the metallic droplets impinged on the substrate is cooled down by the cooling plate and becomes the spray forming material. The rest of the metallic droplets leaves the substrate and is further solidified to the metal powder in the spray chamber. The precipitation rate of the metallic spray on the substrate is controlled by the diameter of the substrate, D, the height of the substrate ring, hp, and the separation distance from the outlet of the atomizer to the substrate, H. This in turn determines the powder production rate and the particle size of the metal powder. In this paper, we used the substrate with D=10 cm. Experiments are performed with hp varying from 0 to 3.0 cm and the separation distance of the substrate and the atomizer varying from 20 cm to 40 cm. The working medium used in this research is Sn63Pb37 eutectic metal. The melting point of the eutectic metal is 183°C. The metal powder is collected at the bottom of the spray chamber and measured by a Malvern RT-Sizer This measurement is based on the Fraunhofer diffraction technique. The laser beam is expanded to a beam diameter of 5 mm in the transmitter and is diffracted by the particles when passing through the powder cloud. The diffracted light is received by the photo detector through the Fourier lens and transferred to digital signal by the A/D converter. And finally, the software of the processor calculates the droplet size distribution.

Fig. 2~4 show the schematic of the atomizers utilized in this research program. Fig. 2 first illustrates the structure of the linear internal-mixing atomizer. The cross section of the atomizer slit is rectangular with aspect ratio ranges from 1.0 to 12. A delivery tube conducts the molten metal to the mixing chamber of the atomizer. The nitrogen gas is introduced into the mixing chamber through the nitrogen supply line located at two sides of the nozzle assembly. Fig. 3 shows the schematic of the atomizer with swirling design. A delivery tube conducts the melt to the mixing chamber of the atomizer. The nitrogen gas is introduced into the mixing chamber through the nitrogen

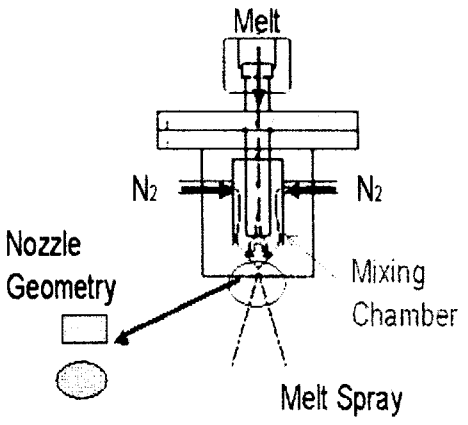

Fig. 2 Schematic of the linear internal-mixing atomizer

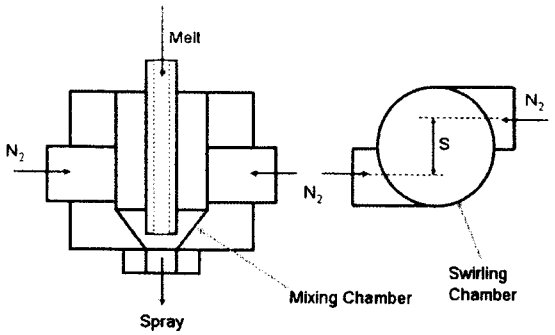

Fig. 3 Schematic of the internal-mixing atomizer with swirling effect

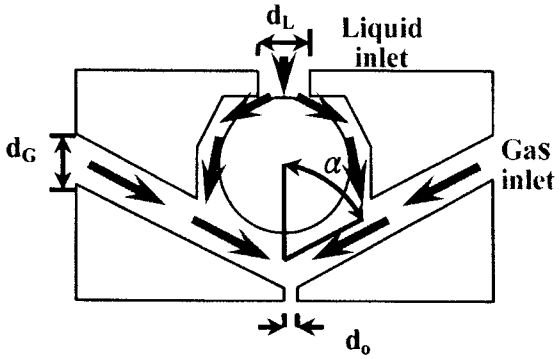

Fig. 4 Schematic of the atomizer with internal impingement

supply line located at two sides of the nozzle assembly. The gas supply lines have a offset of S to create the swirling effects to the two phase flow. The flow rates of the molten metal and the atomization gas can be adjusted to provide the required gas/liquid mass ratios. Fig. 4 shows the schematics of the atomizer with internal impingement. The melt is first injected at the distributor. It results in two streams of the metallic spray flows. They are further introduced to the mixing chamber of the atomizer with flow impingement. The secondary atomization processes takes place when the above two streams come together. Finally, the two phase flow is injected through the orifice for further atomization.

3. Results and discussion

3.1 Performance of a linear atomizer with internal mixing

Fig. 5 illustrates the dependence of d_{32} on the mass

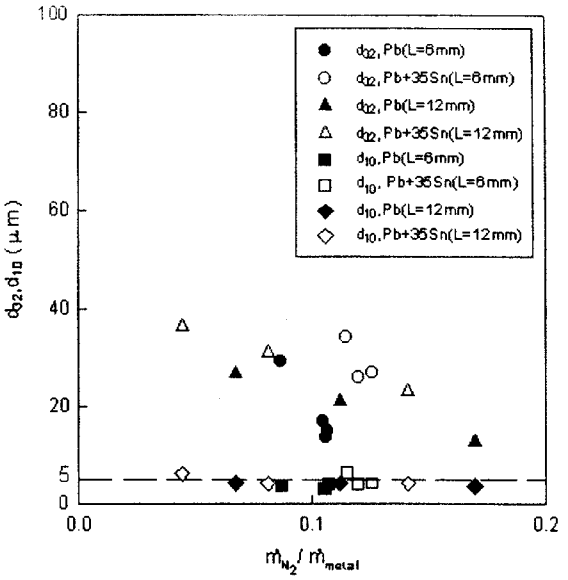

Fig. 5 Dependence of metal powder on mass flow ratio

flow ratio ($\dot{m}_{N_2}/\dot{m}_{metal}$) for the molten metals. As can be seen from this figure, this process is a quite efficient atomization process. For example, as the mass flow ratio $\dot{m}_{N_2}/\dot{m}_{metal}$ increases from 0.04 to 0.17, d_{32} decreases from 27 mm to 13 mm for Pb and it decreases from 37 mm to 23 mm for Pb65Sn35 alloy. It seems that the d_{32} depends on the properties of the molten metal because the density and the over heated temperature of the molten metal are different for these two cases. The densities of the pure Pb and Pb65Sn35 alloy are 11.30 g/cm^3 and 9.9 g/cm^3, respectively. It turns out that the atomization performance is better with the higher density in molten metal atomization. However, the molten points are 330°C and 231.9 for Pb and Sn, respectively. When they are operated at the same temperature for both cases, the overheating temperature of Pb65Sn35 alloy is much higher than Pb metal. Hence the higher overheating temperature of the molten metal is not the important factor in determining the atomization performance within the test range.

Fig. 6 further compares the dependence of the liquid mass flow rates on its supply pressure. As can be seen from this figure, the mass flow rates of the molten metals remain almost constant even when their pressures have been changed from 1 kg/cm^2 to 5 kg/cm^2. For example, the mass flow rate of Pb is about 3.6 kg/min

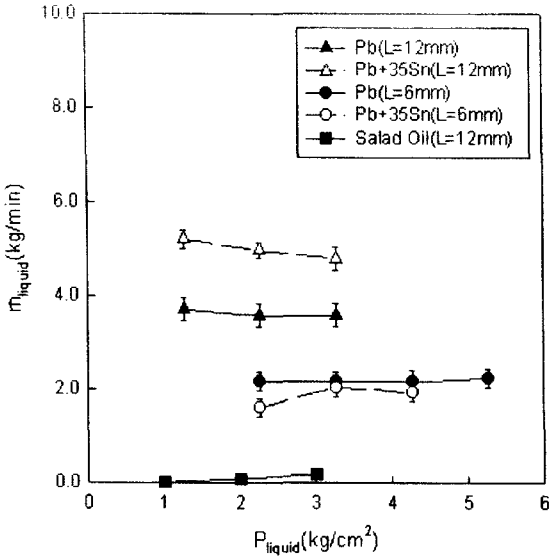

Fig. 6 Dependence of the mass flow rates of melt on the supply pressure

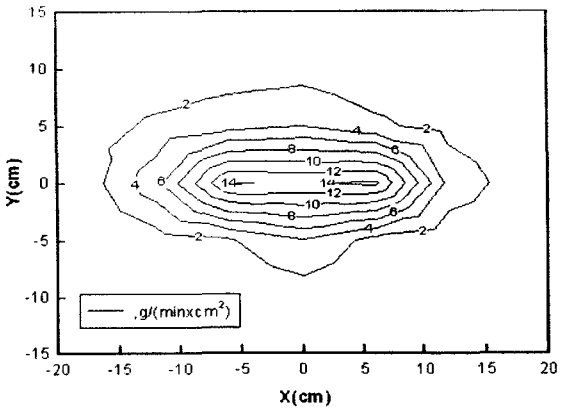

Fig. 7 Mass flux distribution of the Pb and 65Pb35Sn sprays (orifice:1 mm × 12 mm P_{metal}=2.27 bar, P_{N_2}=3 bar)

Fig. 8 The contour of the deposited material

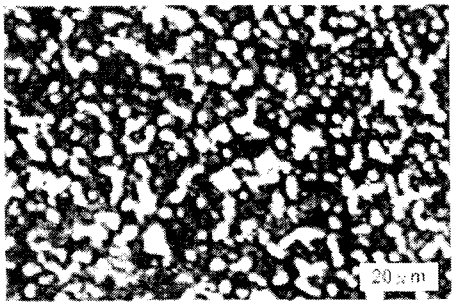

Fig. 9 Microstructure of Pb65Sn35 deposit (Magnification; 1: 550)

as the pressure varies from 1.27 kg/cm^2 to 3.27 kg/cm^2 for the case of L=12 mm. Similar result happens to the Pb65Sn35 alloy with a mass flow rate about 5.0 kg/min under the same conditions. When the orifice length reduces to L=6 mm, the mass flow rates also decrease. For example, the mass flow rate of Pb remains 2.2 kg/min as the pressure varies from 2.27 kg/cm^2 to 5.27 kg/cm^2 for the case of L=6 mm. Similar result happens to the Pb65Sn35 alloy with a mass flow rate of 2.0 kg/min under the same conditions (L=6 mm). It seems clear that the supply pressure of the molten metal is not a control parameter in the spray forming process. This result is quite different from that of the oil, indicating a special mechanism involved in the atomization of the molten metals. It is suggested that the performance of the atomizer is enhanced due to the high temperature mixing process in the mixing chamber. However, the above results also indicate that the metal mass flow rate can be controlled through the adjustment of the orifice length that is a design parameter of the atomizer.

The patternation measured at the position 30 cm from the atomizer is used to characterize the distribution of the metallic spray. Fig. 7 shows the typical mass flux distribution of the Pb and Pb65Sn35 alloy collected at the substrate. The pattern of the mass flux distribution looks like a long ellipse as we expected from a slit type nozzle design. This spray pattern, in turn, results in a metal deposit with 25 cm in length and 15 cm in width when it is collected on the substrate located at a position 30 cm from the atomizer. The mass flux distribution decreases from 20 g/(min×cm^2) in the central region to 0 g/(min×cm^2) at the outer region with a uniform ramping rate 4 g/(min×cm^2). Fig. 8 further illustrates the cutout of the material. These characteristics should be useful in the two dimensional spray forming applications.

Fig. 9 further illustrates the microstructures of the Pb65Sn35 deposit. The specimen was etched to show

the microstructures of the deposit. As can be seen from this figure, the microstructures of the deposit are quite uniform with fine grain size of the material. The measure of the distance between the primary Pb phase and the eutectic phase is about 5 mm.

3.2 Production of metal powder by a linear atomizer with low aspect ratio

Fig. 10 shows that the mean powder size(SMD) reduces from 32.79~39.92 μm to 19.87~22.87 μm as ΔGP increases from 30 kPa to 120 kPa, under different aspect ratios of the orifices. It seems that high performance can be achieved with a relatively low atomization pressure. For example, the mean particle size of metal powder less than 20 μm is achieved under an atomization pressure of 520 kPa. Fig. 5 and 6 also indicate that SMD reduces from 32.79 μm to 21.83 μm

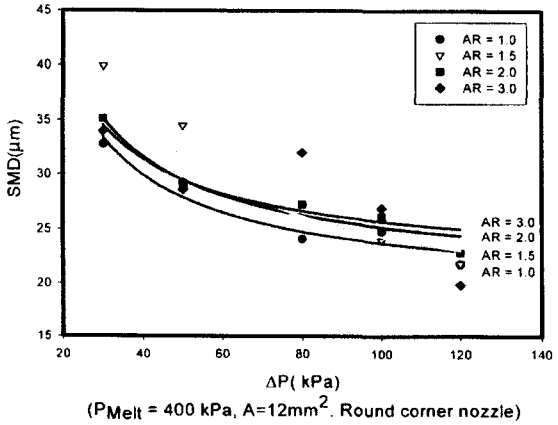

Fig. 10 Dependence of SMD on ΔP

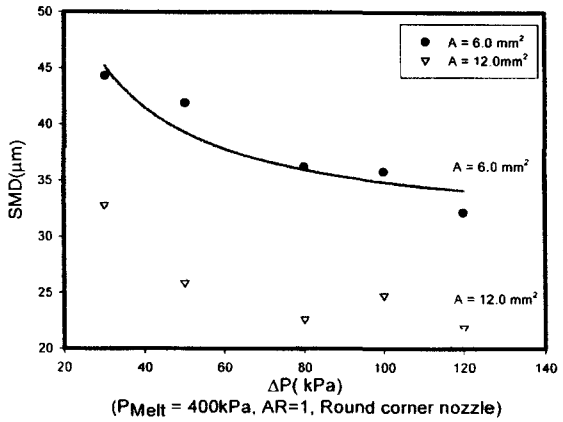

Fig. 11 Dependence of SMD on orifice area

as the GMR increases from 0.04 to 0.08. In contrast, as reported in the literature, GMR's using external-mixing atomizers are normally in the range of 1.0 to 2.0[3].

Hence, the proposed atomizer exerts greater atomization efficiency than traditional ones.

The cross sectional area of the orifice is a design point of the atomizer. It determines the flow rate of the melt and atomization gas. Two cases are compared in the tests: one with orifice area of 6 mm^2 and the other with orifice area of 12 mm^2, denoted by orifice-6 and orifice-12, respectively. Fig. 11 demonstrates the influence of the orifice area the particle size. As expected, orifice-12 achieves better atomization performance in terms of the particle size. As shown in Fig. 11, SMD with orifice-12 reduces from 32.79 μm to 21.83 μm as ΔP increases from 30 kPa to 120 kPa. On the other hand, SMD with orifice-6 is in the size range of 44.27 μm to 32.18 μm. The particle size further reduces to 16.01 μm as the orifice area is increased to 24 mm^2

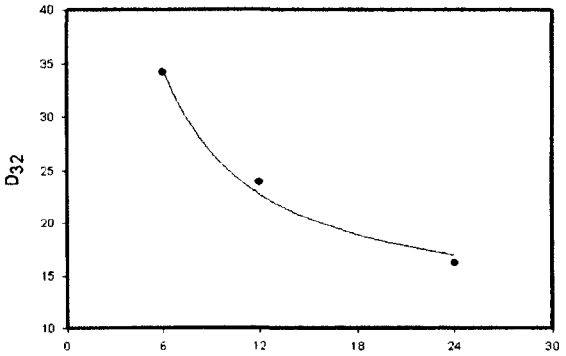

Fig. 12 Dependence of SMD on Orifice Area (P=400 kPa, ΔP =80 kPa, AR=1.0)

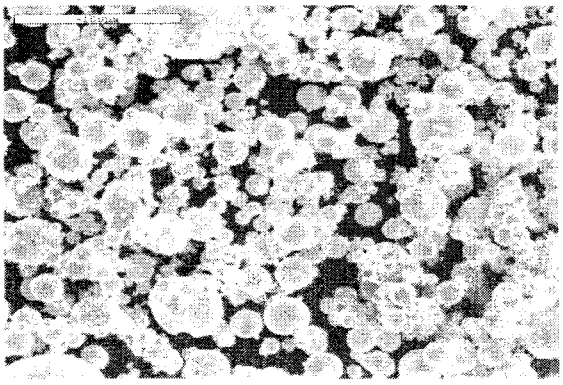

Fig. 13 Scanning electron micrographs of metal powders

(see Fig. 12). The micrograph of the metal powder is shown in Fig. 13. Very fine and spherical metal powder has been produced by this process. Note that this performance can only be achieved under much higher atomization pressure by the conventional atomizers.

3.3 Production of metal powder by internal impingig atomizer

Fig. 14 illustrates the dependence of the particle size on the gas-to-melt-mass ratio in a test program using the internal impinging atomizers (see Fig. 4). Totally 54 test runs with injection pressure ranging from 1.5 bar to 5.0 bar. were carried out in the experiments. As can be seen from this figure, the mean particle size of the metal powder was decreased from 22 μm to 12 μm as the gas-to-melt-mass ratio increased from 0.05 to 0.22. It indicates that the ultra-fine powder can be obtained under this particular design.

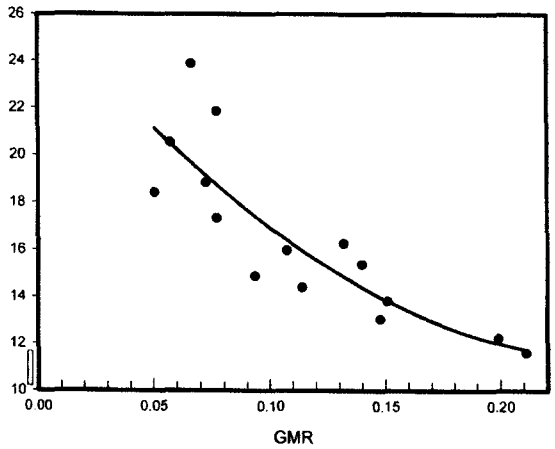

Fig. 14 Dependence of the particle size on the gas-to-melt-mass ratio

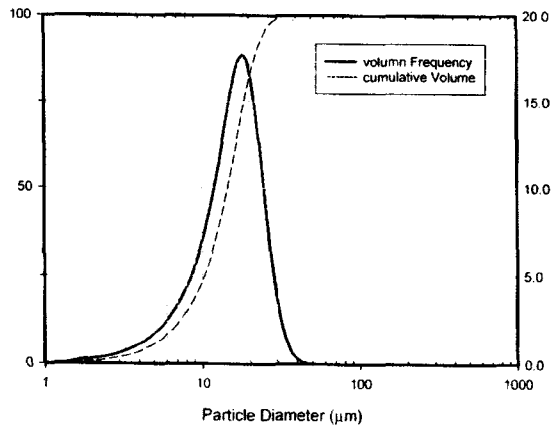

Fig. 15 Particle Distribution of the metal powder produced by Internal-impinging Atomizer

The particle distribution of the metal powder is further shown in Fig. 15. The size distributions is quite uniform. Almost all the particles are below 30 μm. It can be used in the chip scaled packing applications.

3.4 Atomization performance of atomizer with a substrate

Fig. 16 shows the dependence of the mean particle size of the metal powder on the separation distance between the substrate and the atomizer. Experiments are performed with h_p = 0 cm. The particle size of the metal powder increases from 3.13 μm to 12.82 μm as the substrate is moved from 20 cm to 40 cm from the atomizer. It indicates that the adjustment of the location of the substrate can be used to control the particle size of the metal powder. It also justifies that particle size as low as 3 μm can be obtained. None of the result has been reported in the literature of the gas atomization processes. Hence it can be used to produce the ultra-fine powder because the larger molten droplets in the spray jet are deposited on the substrate during the two phase impinging processes. Only the fine particles are able to escape from the impinging flow region near the substrate.

Furthermore, the solidification processes of the molten droplets take place during the flight in the spray chamber. More droplets will be solidified in the flow

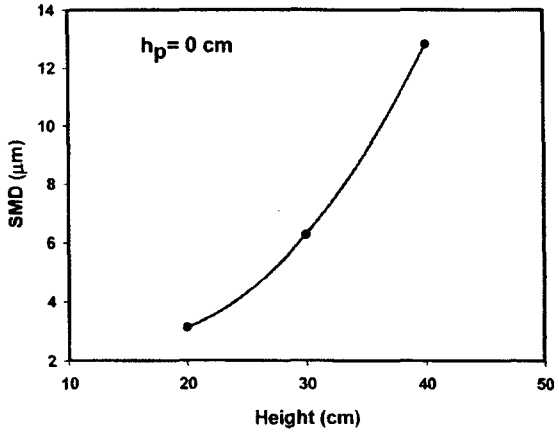

Fig. 16 Dependence of mean particle size on the distance of substrate from the atomizer (D=10 cm, h_p=0 cm)

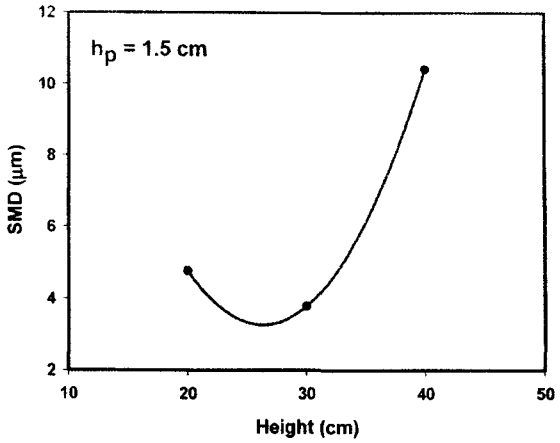

Fig. 17 Dependence of mean particle size on the distance of substrate from the atomizer (D=10 cm, h_p=1.5 cm)

and will not be deposited on the substrate when the substrate is far away from the atomizer. Hence only the portion of the biggest particles would be deposited on the substrate and other portion of the particles will be escaped from the substrate. This explains the reason why the particle size of the metal powder increases as the substrate is moved to the down stream of the spray jet.

The height of the substrate ring can be used to control the particle size of the metal powder as well. For example, Fig. 17 shows that the particle size of the metal powder changes from 3.79 μm to 10.43 μm as the height of the substrate ring increases to h_p=1.5 cm and the substrate is moved from 20 cm to 40 cm. Since the larger particles are easier to deposit on the substrate as hp increases from h_p=0.

Similar result happens when the height of the substrate ring is further increased to h_p=3.0 cm (see Fig. 18). As can be seen from this figure, the particle size of the metal powder is further reduced from 4.44 μm to 6.01 μm as the substrate is placed at 20 cm to 40 cm from the atomizer. It can be concluded that the height of the substrate ring can be used to control the particle size of the metal powder and produce extra-fine metal powder for future applications.

Fig. 19 and Fig. 20 illustrate the production rate of the metal powder and the spray forming material with different substrate designs. Results show that the deposition rate of the spray forming material decreases as the distance between the substrate and the atomizer increases. For example, the deposition rate decreases

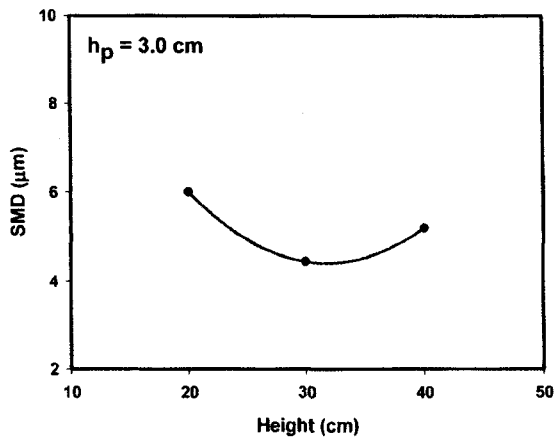

Fig. 18 Dependence of mean particle size on the distance of substrate from the atomizer (D=10 cm, h_p=3.0 cm)

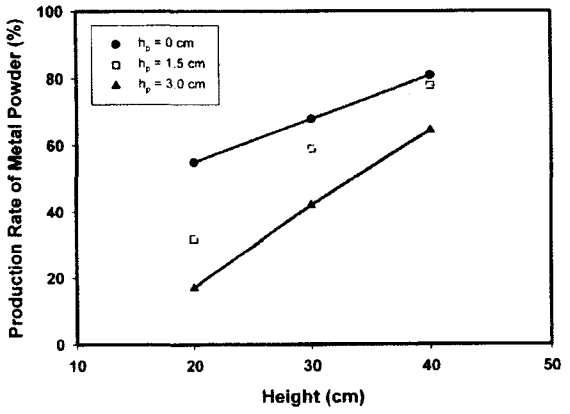

Fig. 19 Production rate of metal powder

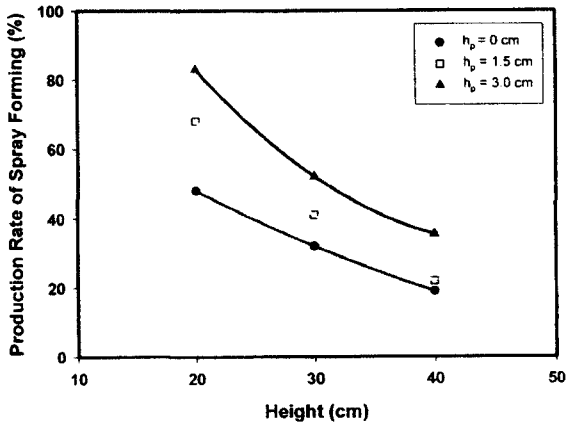

Fig. 20 Production rate of spray forming material

from 48% to 19% as the substrate is placed at a distance from 20 cm to 40 cm. On the other hand, the metal powder production rate and its particle size increases as the substrate is placed far away from the atomizer. For example, the metal powder production rate increases from 52% to 81% as the substrate is placed at 20 cm to 40 cm from the atomizer.

4. Conclusion

Experimental results of the production of metal powder demonstrate the feasibility to produce the ultra-fine powders utilized the atomizers with internal mixing mechanisms. The atomizer coupled with a substrate design show the capacity to produce the metal powder and the spray forming materials simultaneously. Experimental results indicate that the deposition rate of the spray forming material decreases as the distance between the substrate and the atomizer increases. For example, the precipitation rate decreases from 48% to 19% as the substrate is placed at a distance from 20 cm to 40 cm. On the other hand, the metal powder production rate and its particle size increases as the substrate is placed far away from the atomizer. For example, the metal powder production rate increases from 52% to 81% as the substrate is placed at 20 cm to 40 cm from the atomizer. The production of ultra-fine metal powder with mean particle size as low as 3.13 μm has been achieved.

Acknowledgement

This research was supported by National Science Council and Ministry of Economy of Republic of China under contract No. NSC93-2212-E-006-044 and DPA92-EC-17-A-05-SI-0014. Funding from the Center for Micro/Nano Technology Research, National Cheng Kung University, under projects from the Ministry of Education and the National Science Council (NSC 93-212-M-006-006) of Taiwan is highly acknowledged.

References

(1) Cubberly, W.H., Stedfeld, R.L., Mills, K., Davis, J.R., Refsnes, S.K., Sanders, B.R., Frissell, H.J. and Jenkis, D.M., "Metal Handbook ninth edition", Volume 7, Powder Metallurgy, American Society for Metals, 1984.

(2) Lavernia, E.J. "Atomization of alloy powders", Atomization and Sprays 2 (1992), pp. 253~274.

(3) Bradbury, S., "Powder Metallurgy Equipment Manual 3rd edition", Powder Metallurgy Equipment Association, Library of Congress Catalog No.76-523-33 ISBN0-918404-68-1.

(4) German, R.M., "Powder Metallurgy Science", Metallurgy Industies Federation, ISBN 957-584-368-1, 1994.

(5) Liang, X., Earthman, J.C. and Lavernia, E.J., "On the Mechanism of grain Formation During Spray Atomization and Deposition", Acta Metal Mater., Vol. 40, No. 11, 1992, pp. 3003~3016.

(6) Zhou, Y., McDonell, V.G, Samuelsen, G.S., Kozarek, R.L., and Lavernia, E.J., "Size Distribution of Spray Atomized Aluminum Alloy Powders Produced During Linear Atomization", Materials Science and Technology, Vol. 15, No. 2, 1999, pp. 226~234.

(7) Anderson, I.E., and Terpstra, R.L., "Progress Toward Gas Atomization Processing with Increased Uniformity and Control", Material Science and Engineering, A326, 2002, pp. 101~109.

(8) Ting, J., Peretti, M.W. and Eisen, W.B., "The Effect of Wake-Closure Phenomenon on Gas Atomization Performance", Materials Science and Engineering, A326, 2002, pp. 110~121.

(9) Mates, S.P. and Settles, G.S., "High-Speed Imaging of Liquid Metal Atomization by Two Different Closed-Coupled Gas Atomization Nozzles", 1996 World Congress on Powder Metallurgy and Particulate Materials, Washington DC, June 16-21, 1996.

(10) Wang, M.R., Sheu M.S. and. Yang S.R, "Performance of A Linear Internal Mixing Atomizer in Atomization of Molten Metals", Eighth Internal Conference On Liquid Atomization and Spray Systems, Pasadena, CA, USA, July, 2000

(11) Wang, M.R., Lin, T.C., Yang, C.J., Kuo, Z.Z., Sheu, M.S., "Effects of Operating Conditions on Molten Metal Atomization in a Linear Internal Mixing Atomizer", The 7th Annual Conference on Liquid Atomization and Spray Systems- Aisa, Nov. 14-16, 2002, Tainan, Taiwan, ROC

(12) Wang, M.R., Lai, T.S., Lin, T.C., Chiu, C.H., Yang, C.J. and Sheu, M.S., "Optimization of Metal Powder Production by Gas Atomization Processes With Internal-Mixing Mechanism", Transactions of the Aeronautical and Astronautical Society of the Republic of China, Vol. 37, No. 2, 2005, pp. 153~162.

(13) G. Wolf and H.W. Bergmann, Materials Science and Engineering, A326, 2002, pp. 134.

(14) M. Angioletti, R.M.Di Tommaso, E. Nino, G. Ruocco, "Simultaneous visualization of flow field and evaluation of local heat transfer by transitional impinging jets". International Journal of Heat and Mass Transfer 46 (2003), pp. 1703~1713.

(15) Singer, A. R. E., "Aluminum and Aluminum Alloy Strip Produced by Spray Deposition and Alloy", J. Inst. Met., Vol. 100, 1972, pp. 185~190.

(16) Lavernia, E.J., and Wu, Y., "Spray atomization and Deposition", John Wiley & Sons, 1996.

(17) Newbery, A.P., Rayment, T. and Grant, P.S., "A particle image velocimetry investigation of inflight and deposition behaviour of Steel Droplets during electric arc spray forming", Materials Science and Engeering A 383, 2004, pp. 137~145.